Organic Alternatives to Quantum Dots for Intraoperative Near-Infrared Fluorescent Sentinel Lymph Node Mapping

Shunsuke Ohnishi [1], *Stephen J. Lomnes* [2], *Rita G. Laurence* [3], *Andrew Gogbashian* [3], *Giuliano Mariani* [4], *and John V. Frangioni* [1]

[1]Beth Israel Deaconess Medical Center, Boston, MA, [2]General Electric Corporation, Niskayuna, NY, [3]Brigham and Women's Hospital, Boston, MA, and [4]University of Pisa Medical School, Pisa, Italy

Abstract

Intraoperative near-infrared (NIR) fluorescence imaging provides the surgeon with real-time image guidance during cancer and other surgeries. We have previously reported the use of NIR fluorescent quantum dots (QDs) for sentinel lymph node (SLN) mapping. However, because of concerns over potential toxicity, organic alternatives to QDs will be required for initial clinical studies. We describe a family of 800 nm organic heptamethine indocyanine-based contrast agents for SLN mapping spanning a spectrum from 775 Da small molecules to 7 MDa nanocolloids. We provide a detailed characterization of the optical and physical properties of these contrast agents and discuss the advantages and disadvantages of each. We present robust methods for the covalent conjugation, purification, and characterization of proteins with tetra-sulfonated heptamethine indocyanines, including mass spectroscopic site mapping of highly substituted molecules. One contrast agent, NIR fluorescent human serum albumin (HSA800), emerged as the molecule with the best overall performance with respect to entry to lymphatics, flow to the SLN, retention in the SLN, fluorescence yield and reproducibility. This preclinical study, performed on large animals approaching the size of humans, should serve as a foundation for future clinical studies. *Mol Imaging* (2005) **4,** 172–181.

Keywords: Near-infrared fluorescence, intraoperative imaging, sentinel lymph node mapping, fluorophore conjugation, albumin, indocyanine green, mass spectroscopy.

Introduction

The sentinel lymph node (SLN) hypothesis, advanced by Morton and colleagues in the early 1990s [1], states that sampling of the first lymph node to receive lymphatic drainage from a solid tumor is sufficient to assess for the presence or absence of lymphatic metastasis. If no malignant cells are found in the SLN, the patient is spared the morbidity of radical lymph node dissection. SLN mapping has revolutionized the intraoperative staging of many solid tumors, and is now the standard of care in breast cancer and melanoma (reviewed in Ref. [2]).

Presently, SLN mapping is performed with a combination of preoperative radiocolloid injection (e.g., technetium-99m sulfur colloid) and intraoperative injection of a visible blue dye (e.g., isosulfan blue). The radioactive tracer, in conjunction with a handheld gamma probe, improves detection rate and confirms complete resection of the SLN, whereas the colored dye helps locate the SLN [3]. Unfortunately, it is estimated that up to 60 cases are required for technical proficiency for breast cancer SLN mapping [4], and in published series without a high number of learning cases per surgeon, up to 16% of SLNs were missed [5]. When also considering that the technique requires radioactivity, and that the blue dye is extremely difficult to see in the presence of blood or anthracosis, technological innovation is clearly needed.

Owing to high photon penetration and low autofluorescence in the 700 to 900 nm wavelength range, near-infrared (NIR) light is considered favorable for in vivo imaging (reviewed in Refs. [6–8]). Our laboratory has previously developed intraoperative NIR fluorescence imaging systems that permit anatomy (color video) and function (NIR fluorescence) to be acquired simultaneously and in real time [9,10]. We have also demonstrated the use of inorganic/organic hybrid quantum dots (QDs) for NIR fluorescent SLN mapping in the skin [11], lung [12], esophagus [13], and pleural space [14] (reviewed in Ref. [15]). However, because current formulations of QDs include potentially toxic heavy metals, the purpose of this study was to develop and evaluate purely organic alternative contrast agents, which have a higher likelihood of eventual clinical use.

There are three key design features of a lymphatic tracer for SLN mapping: hydrodynamic diameter, surface

Abbreviations: DMSO, dimethylsulfoxide; ES-TOF, electrospray time-of-flight; FBS, fetal bovine serum; HSA, human serum albumin; ICG, indocyanine green; LC/MS, liquid chromatography/mass spectrometry; MALDI-TOF, matrix-assisted laser desorption ionization time-of-flight; NHS, *N*-hydroxysuccinimide; NIR, near infrared; PBS, phosphate-buffered saline; QDs, quantum dots; RT, room temperature; SLN, sentinel lymph node; QY, quantum yield.

Corresponding author: John V. Frangioni, Beth Israel Deaconess Medical Center, Room SL-B05, 330 Brookline Avenue, Boston, MA 02215; e-mail: jfrangio@bidmc.harvard.edu.

Received 10 March 2005; Received in revised form 18 April 2005; Accepted 22 April 2005.

charge, and contrast generation. Molecules with a hydrodynamic diameter less than approximately 10 nm have the potential to travel beyond the SLN, molecules with a 50–100 nm hydrodynamic diameter require up to 3 hr to label the SLN, and very large molecules (>200 nm) require up to 24 hr to label the SLN [16]. Anionic molecules have rapid uptake into lymphatics and excellent retention in lymph nodes [17,18]. In this study, we present five anionic, purely organic, 800 nm fluorescent formulations that can be used for SLN mapping: (1) indocyanine green (ICG); (2) CW800-CA, the carboxylic acid of the novel tetra-sulfonated heptamethine indocyanine CW800; (3) ICGHSA, a noncovalent adsorption of ICG to human serum albumin (HSA); (4) HSA800, a covalent conjugate of CW800 to HSA; and (5) Nanocoll800, a covalent conjugate of CW800 to HSA nanocolloid. We compare the physical and optical properties of these organic contrast agents to NIR QDs, and measure their performance during SLN mapping of large animals approaching the size of humans.

Materials and Methods

Reagents

The NHS ester (CW800-NHS) and carboxylic acid (CW800-CA) forms of IRDye™ 800CW NIR dye were dry powders from LI-COR (Lincoln, NE). They were resuspended to 30 mM in DMSO (Sigma, St. Louis, MO) under reduced light conditions and stored at −80°C. ICG was purchased from Sigma, resuspended to 10 mM in DMSO and stored at −80°C. Human albumin nanocolloid (Nanocoll™) was from Amersham Health (Milan, Italy). HSA 25% solution (ZLB Bioplasma AG, Berne, Switzerland) was purchased from the American Red Cross (Washington, DC). NIR QDs were produced as previously described [11] and stored as a 5.7 μM solution in phosphate-buffered saline (PBS), pH 7.4.

Noncovalent Adsorption of ICG to HSA

The adsorption of ICG to HSA was performed essentially as described previously [19]. ICG and HSA were added to a solution of PBS, pH 7.8 to a final concentration of 10 μM each (1:1 molar ratio), vortexed at low speed for 20 sec at RT, and stored on ice until used.

Covalent Conjugation Reactions

All steps were performed under reduced light conditions. Covalent conjugation reactions contained 7.5 mg/mL HSA or 10 mg/mL Nanocoll and various molar ratios of CW800-NHS in PBS, pH 7.8. Reaction volumes ranged from 100 μL (analytical) to 10 mL (preparative). Conjugation was initiated by adding CW800-NHS, and constant agitation (without frothing) was continued for 2 hr at RT.

Gel Filtration Chromatography and Absorbance/Fluorescence Spectrometry

The gel filtration chromatography system consisted of an ÄKTA prime pump with fraction collector (Amersham Biosciences, Piscataway, NJ) and an Econo-Pac P6 chromatographic cartridge with a cutoff of 6000 Da (Bio-Rad, Hercules, CA). On-line absorbance spectrometry was performed with a model 75.3-Q-10, 1-cm path length, 70 μL quartz flow cell (Starna, Atascadero, CA), USB2000 fiber-optic spectrometer, and CHEM2000–UV–VIS light source with cuvette holder (Ocean Optics, Dunedin, FL). On-line fluorescence spectrometry was performed with a model 583.4.2F-Q-10, 1-cm path length, 80 μL flow cell (Starna), HR2000 fiber-optic spectrometer, and CUV-ALL-UV four-way cuvette holder (Ocean Optics), and 770 nm NIR laser diode light source (Electro Optical Components, Santa Rosa, CA) set to 8 mW and coupled through a 300-μm core diameter, NA 0.22 fiber (Fiberguide Industries, Stirling, NJ). Data acquisition was performed with two Dell computers using the OOIBase32 spectrometer operating software package (Ocean Optics). The spectral range of USB2000 spectrometer was from 200 to 870 nm with a spectral resolution of 1 nm, and that of HR2000 spectrometer was from 200 to 1100 nm with a spectral resolution of 6.7 nm.

After conjugation, the sample was loaded into the injector and run at a flow rate of 1 mL/min using PBS, pH 7.8 as mobile phase. Full-spectrum absorbance and fluorescence data were recorded every 10 sec. Desired products were collected by the fraction collector, pooled, and stored at 4°C in the dark until use without preservatives. The labeling ratio and the concentration of the conjugated protein were estimated using the extinction coefficients of HSA (ε_{280nm} = 32,900 M^{-1} cm^{-1}) and CW800-CA (ε_{785nm} = 240,000 M^{-1} cm^{-1}) in PBS, with correction for the 6.5% of measured absorbance at 280 nm due to CW800-CA:

$$\text{Labeling Ratio} = (\text{Abs}_{785nm}/\varepsilon_{785nm})/((\text{Abs}_{280} - 0.065 * \text{Abs}_{785nm})/\varepsilon_{280nm})$$

QY Measurements

QYs of contrast agents in PBS, pH 7.8 or 100% fetal bovine serum (FBS) were calculated using ICG in DMSO

(QY 13%; [20]) as calibration standard, under conditions of matched fluorophore absorbance.

MALDI-TOF Mass Spectrometry

Molecular weights of intact HSA and HSA800 were measured using matrix-assisted laser desorption ionization time-of-flight (MALDI-TOF) mass spectrometry on a Voyager-DE (Applied Biosystems, Foster City, CA). One microgram of protein in PBS, pH 7.8 was desalted with $ZipTip_{C4}$ pipette tips (Millipore, Billerica, MA), equilibrated with 100% acetonitrile, 50% acetonitrile with 0.05% trifluoroacetic acid (TFA), and 0.1% TFA sequentially. Samples were loaded with the matrix 3, 5-dimethoxy-4-hydroxycinnamic acid (sinapinic acid), and the mass spectrum was obtained from 100 shots using positive reflector mode and a laser intensity of 2600–2800 V, with a spectral range of 60,000–80,000 Da. Data were analyzed with Data Explorer (Applied Biosystems) software.

ES-TOF Mass Spectroscopic Site Mapping

Two hundred thirty microliters of 8 M urea/400 mM ammonium bicarbonate solution was added to 400 μg HSA or HSA800 in 20 μL of PBS, pH 7.8, 5 μL of 45 mM DTT was added and incubated 15 min at 50°C, and 5 μL of 100 mM iodoacetamide was added and incubated for 15 min at RT. The mixture was diluted with 750 μL of buffer (80 mg ammonium bicarbonate and 6 mg $CaCl_2$ in 10 mL H_2O), 20 μg of TPCK-trypsin (L-1-tosylamide-2-phenylethyl ketone-treated, Sigma, catalog #T1426) was added, and the solution was incubated 24 hr at 37°C. Twenty-five microliters of this peptide digest was used for analysis on a Waters (Milford, MA) LCT ES-TOF LC/MS equipped with dual-absorbance detectors, a Sedex Model 75 evaporative light scatter detector (ELSD; Richards Scientific, Novato, CA), and a lock-spray. Absorbance detectors were set to 254 and 700 nm (the maximum permitted wavelength). Bovine heart myoglobin (5 μM) in water was used as a mass reference. Buffer A was 10 mM triethylammonium acetate, pH 7 (Glen Research, Sterling, VA) and Buffer B was acetonitrile. Peptides were resolved on a 4.6 × 150 mm Symmetry (Waters) C_{18} column at a flow rate of 1 mL/min, using a gradient of 0% to 50% B over 40 min. Data were analyzed with MassLynx (Waters) software, and expected peptide masses were calculated from the mass obtained from Peptidemass (http://au.expasy.org/tools/peptide-mass.html) with the addition of the mass of CW800-CA (1000.17) and subtraction of the mass of H_2O (18.02). 3-D protein structure was visualized on a Macintosh iMac computer running RasMac Molecular Graphics version 2.6-ucb1.0 (University of California, Berkeley, CA).

SLN Mapping and Resection

Animals were housed in an AAALAC-certified facility staffed by full-time veterinarians, and were studied under the supervision of an approved institutional protocol. This protocol adhered to the ''NIH Principles for the Utilization and Care of Vertebrate Animals Used in Testing, Research, and Training.'' Yorkshire pigs of either sex were purchased at 35 kg from E. M. Parsons and Sons (Hadley, MA). All animals acclimated to the animal facility for at least 48 hr prior to experimentation. After each study, anesthetized animals were euthanized by rapid intravenous injection of 10 mL of Fatal-Plus (Vortech Pharmaceuticals, Dearborn, MI). This method of euthanasia is consistent with the recommendations of the Panel on Euthanasia of the American Veterinary Medical Association.

The intraoperative NIR fluorescence imaging system optimized for large animal surgery [10] has been described in detail previously. Briefly, it is composed of two wavelength-isolated excitation sources, one generating 0.5 mW/cm^2 400–700 nm ''white'' light, and the other generating 5 mW/cm^2 725–775 nm light over a 15-cm diameter field of view. Simultaneous photon collection of color video and NIR fluorescence images is achieved with custom-designed optics that maintains separation of the white light and NIR fluorescence (>795 nm) channels. After computer-controlled (LabVIEW, National Instruments, Austin, TX) camera acquisition via custom LabVIEW software, anatomic (white light) and functional (NIR fluorescence light) images can be displayed separately and merged. All images are refreshed up to 15 times per second. The entire apparatus is suspended on an articulated arm over the surgical field, thus permitting noninvasive and nonintrusive imaging.

The injection technique is critical to the success of SLN mapping. Injection too shallow or too deep into the tissue results in formation of a bleb, but no migration of lymphatic tracer from the site. Optimal technique includes keeping the needle bevel facing upwards, and the syringe at a 45° angle relative to the plane of the tissue. Direct cannulation of lymphatic channels is not necessary. After injection, gentle thumb pressing of the injection site will increase hydrostatic pressure and greatly accelerate lymphatic flow to the SLN. Contrast agents were loaded into a 1-mL syringe equipped with a 25-gauge, 1/2-in. needle and injected into the parenchyma of the tissue under study. Injections into the intestine consisted of 100 μL of 10 μM fluorophore

(1 nmol) of ICG, CW800-CA, ICGHSA, HSA800 (labeling ratio = 3.0), or 4 μM fluorophore (0.4 nmol) of Nanocoll800 (labeling ratio = 2.7), or 0.4 μM (0.04 nmol) of QDs in PBS, pH 7.8. Injections into the foot consisted of 300 μL of 10 μM fluorophore (3 nmol) of ICG, ICGHSA, or HSA800.

Results

Synthesis of HSA800 and Nanocoll800

After reaction of CW800-NHS with HSA or albumin nanocolloid, the product was isolated by gel filtration chromatography to a purity ≥98%. Under our experimental conditions, the labeling ratio was increased as the mixing ratio increased (Figure 1A). However, as the labeling ratio increased, the fluorescence of any single fluorophore decreased when compared with a free CW800-CA molecule in solution (Figure 1B). Optimal per-molecule fluorescence yield for HSA800 and Nanocoll800 was obtained at labeling ratios of ≈4.0, and ≈2.7, respectively (Figure 1C). Due to the sharp decline in fluorescence yield for HSA800 at labeling ratios above 4, HSA with a labeling ratio of 3.0 was used for further study. MALDI-TOF analysis demonstrated that HSA800 is, as expected, a mixture of HSA labeled with various numbers of CW800, and confirmed the accuracy of the calculation of the labeling ratio from the absorbance and extinction coefficient (Figure 2A).

Physical and Optical Properties of a Family of 800 nm Contrast Agents for SLN Mapping

Physical properties and optical properties of the contrast agents analyzed in this study are summarized in Tables 1 and 2, respectively. The hydrodynamic diameters of free ICG and CW800-CA were only 1.2 and 1.3 nm, respectively, whereas ICGHSA and HSA800 were 7.3 and 7.4 nm, respectively. Nevertheless, only Nanocoll800 and NIR QDs had a hydrodynamic diameter that resulted in complete retention by the first lymph node encountered (Table 1). Anionic surface charge, another key parameter for SLN retention, differed markedly among the agents (Table 1). The oligomeric phosphine coating of NIR QDs led to the desired highly anionic surface, although it should be noted that the charge-to-mass ratios of NIR QDs and all organic contrast agents except Nanocoll800 were similar (Table 1).

All contrast agents had reasonable extinction coefficients, and had emission wavelengths compatible with

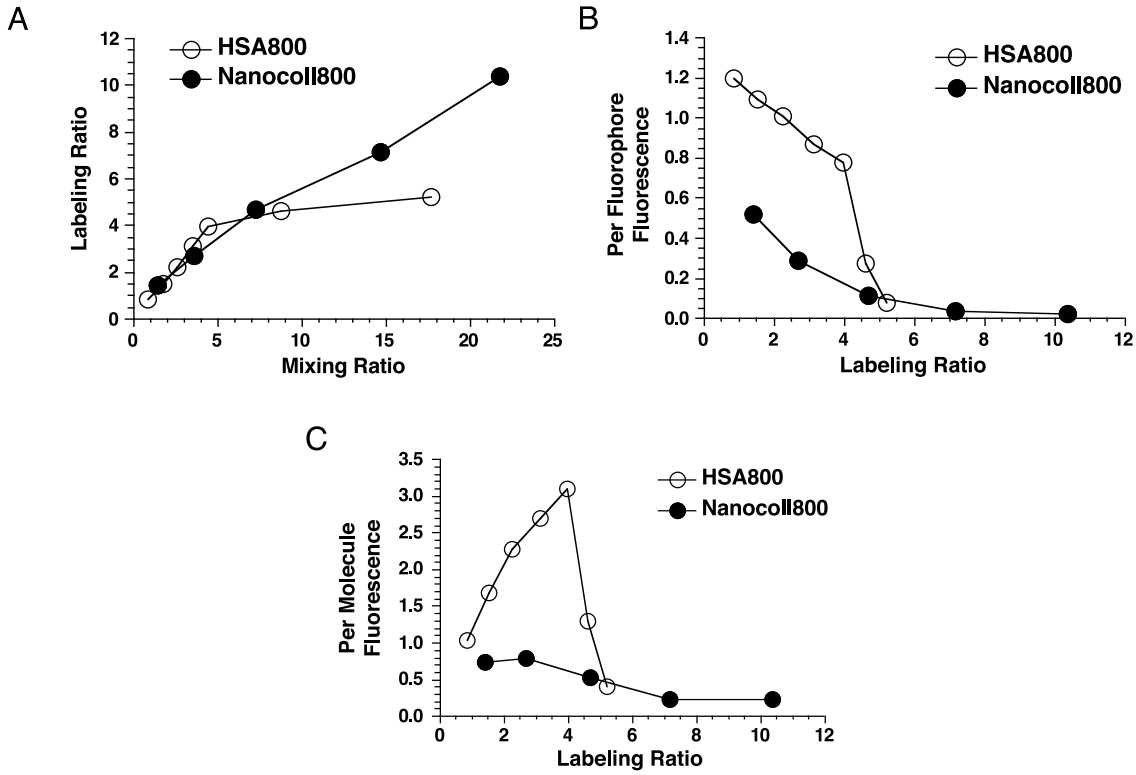

Figure 1. *Optimization of fluorescence yield of HSA800 and Nanocoll800. (A) The fluorophore to protein molar labeling ratio was measured at various fluorophore to protein molar mixing ratios. (B) Per-fluorophore QY, compared to one molecule of CW800-CA, was measured as a function of the labeling ratio. (C) Per-molecule fluorescence yield was calculated from the labeling ratio and per-fluorophore fluorescence, and compared to the same fluorophore concentration (1 μM) of CW800-CA in PBS, pH 7.4.*

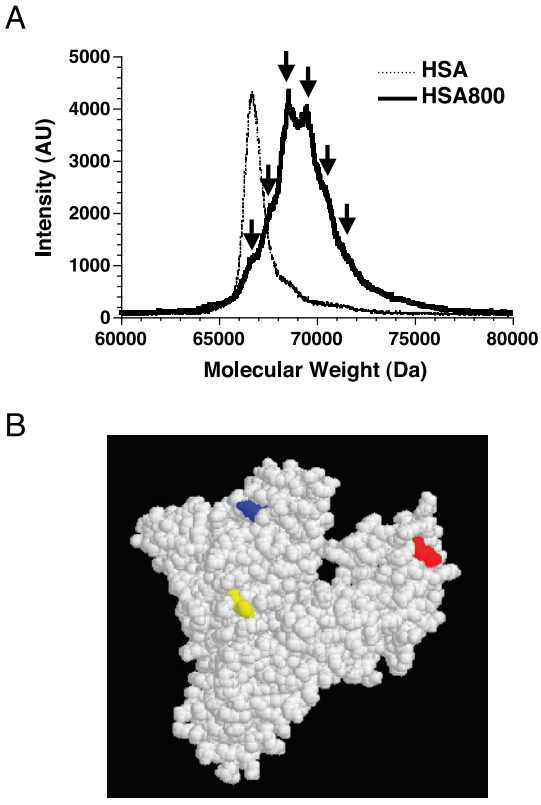

Figure 2. *Mass spectroscopic analysis of HSA800. (A) MALDI-TOF analysis of unlabeled HSA and HSA800 at a labeling ratio of 3.0. HSA800 is demonstrated to be a mixture of proteins with various labeling ratios (arrows), with each one differing by the expected mass of 982 Da. (B) Predicted three-dimensional structure of HSA800. The conjugation sites of CW800 to HSA (white) were established using trypsin digestion and ES-TOF LC/MS peptide analysis. The amino acid substitution sites are: Lys162 (blue), Lys274 (yellow), and Lys557 (red).*

our intraoperative NIR fluorescence imaging system (Table 2). As is typical with heptamethine indocyanines, a slight bathochromatic shift accompanied fluorophore association with proteins (Table 2). Most importantly, the per-fluorophore QY and total fluorescence yield differed markedly among the contrast agents, and was a strong function of chemical environment. For this reason, Table 2 reports all optical parameters in both PBS and, more relevant to in vivo imaging, FBS. As described previously [19,21], for example, the extinction coefficient and QY of ICG were remarkably increased in the presence of high protein concentration (Table 2). Tetra-sulfonated NIR fluorophores, such as CW800, are much less affected by chemical environment.

Tryptic Digestion of HSA800

To determine the precise fluorophore conjugation sites on HSA800, we performed tryptic digestion of HSA800 followed by LC/MS peptide analysis. Three dominant conjugation sites were found (Table 3), with each site located at the surface of the molecule (Figure 2B). Interestingly, the spacing between individual fluorophores was nearly maximal, offering mechanistic insight as to why per-fluorophore QY was preserved despite a high fluorophore-to-protein substitution ratio.

Total Fluorescence Yield as a Function of Concentration

For clinical testing, it is desirable to minimize the injected dose of contrast agent while maximizing its fluorescence yield. This is an important consideration because intermolecular quenching and internal absorption often limit the usable concentration range of a fluorescent contrast agent. We thus examined how total fluorescence yield changed as a function of contrast agent concentration. As shown in Figure 3A, QDs had extremely high fluorescence yield compared with the same concentration of organic fluorophores in PBS. Importantly, even the best organic contrast agents had a fluorescence yield that peaked at a fluorophore concentration of approximately 10 μM in both PBS (Figure 3A) and FBS (Figure 3B), limiting the maximal concentration of injected agent. Above this concentration (4 μM for Nanocoll800), there was actually a decrease in fluorescence yield. It should also be noted that in FBS, this concentration effect was even more pronounced than in PBS.

Intraoperative NIR Fluorescent SLN Mapping

In order to evaluate the performance of these organic contrast agents in vivo, we performed SLN mapping

Table 1. Physical Characteristics of Organic Contrast Agents for SLN Mapping

Contrast agent	M.W. (Da)	Hydrodynamic diameter (nm)	Protein	NIR fluorophore	Net charge at pH 7.4	Charge-to-mass ratio ($\times 10^{-3}$)	Notes
ICG	776	1.2	n/a	Same	−1	−1.2	Hydrophobic disulfonated heptamethine indocyanine
CW800-CA	962	1.3	n/a	Same	−3	−3.1	Water-soluble tetra-sulfonated heptamethine indocyanine
ICGHSA	67K	7.3	HSA	ICG	−20	−3.0	Noncovalent adsorption of ICG to HSA
HSA800	70K	7.4	HSA	CW800	−27	−3.9	Covalent conjugation of CW800 to HSA
QD	400K–800K	15–20	n/a	Same	−500	−0.63 to −1.3	Type II quantum dot with oligomeric phosphine coating
Nanocoll800	7M	4–100 (Avg. 50)	Human albumin nanocolloid	CW800	−26	−0.0037	Covalent conjugation of CW800 to albumin nanocolloid

Table 2. Optical Characteristics of Organic Contrast Agents for SLN Mapping

Contrast agent	Labeling ratio	Extinction coefficient (M^{-1} cm^{-1}) PBS (FBS)	Excitation wavelength maximum PBS (FBS)	Emission wavelength maximum PBS (FBS)	Per-fluorophore QY PBS (FBS)	Per-molecule (2 μM) fluorescence yield compared to ICG in PBS (FBS)
ICG	n/a	110,000 (166,000)	779 (800)	806 (811)	1% (9%)	1.0 (3.7)
CW800-CA	n/a	242,000 (237,000)	775 (783)	796 (801)	9% (12%)	7.4 (9.9)
ICGHSA	1.0	121,000 (169,000)	792 (800)	811 (814)	3% (9%)	1.7 (3.6)
HSA800	3.0	242,000 (237,000)	784 (784)	804 (802)	8% (12%)	6.5 (7.8)
NIRQD	n/a	559,000*(581,000*)	n/a	808 (814)	8% (9%)	17.7 (10.3)
Nanocoll800	2.7	242,000 (237,000)	796 (800)	817 (821)	3% (6%)	2.2 (1.8)

*At first absorption peak of 775 nm.

in pigs approaching the size of humans. Figure 4 shows the SLN mapping of the intestine with a family of 800 nm contrast agents. Due to its poor QY, ICG was extremely difficult to detect, even in the absence of overlying tissue, and was often seen passing through the SLN. Although one might expect an increase in ICG's QY after binding to albumin in lymph, this was never observed. One possibility is that the kinetics of albumin binding are too slow relative to lymph flow, however, the more likely explanation is that albumin is competed by ICG's high affinity for α_1-lipoprotein and γ-globulin [21]. CW800-CA provided higher contrast, but also showed relatively poor retention in the SLN. ICGHSA improves ICG fluorescence and SLN retention dramatically, but still has a twofold lower fluorescence yield than HSA800. Nanocoll800 demonstrated slow uptake into the lymphatics, but had the best SLN retention. HSA800 appeared to have the best tradeoff among entry into the lymphatics, as well as total fluorescence yield and SLN retention.

A more rigorous evaluation of contrast agent performance utilizes the porcine lower limb. In this model, the injection site is at a distance over 25 cm from the SLN, and the SLN itself is located approximately 1 cm below highly scattering tissue [11]. As shown in Figure 5, HSA800 demonstrated ultra-fine lymphatic channels flowing to a single SLN. The SLN could be identified unequivocally and resected under image guidance. However, ICG failed to identify the SLN over this clinically relevant distance. At the relatively low (5 mW/cm^2) excitation fluence rate used in this study, ICGHSA provided enough contrast to visualize subdermal lymphatics, but not quite enough to render SLN identification unequivocal until the initial incision was made (Figure 5).

Table 3. Mass Spectrometry of Peptides of Trypsin-Digested HSA800 (Labeled Lysine Residue Appears in Boldface)

Amino acids	Sequence	Mass (expected/observed)
161–174	Y**K**AAFTECCQAADK	2642.9/2643.0
263–276	YICENQDSISS**K**LK	2665.0/2664.9
558–560	AVMDDFAAFVF**K**CCK	2770.9/2770.8

Discussion

In this study, we report five different organic alternatives to NIR QDs for optically guided SLN mapping. The development of such agents is a necessity for human clinical studies, given the unresolved issues surrounding the potential toxicity of NIR QDs. Each of the agents we describe is composed of potentially nontoxic reactants. We also systemically addressed the factors known to affect lymphatic uptake and retention, such as hydrodynamic diameter, surface charge, and hydrophobicity [17,22,23]. In addition, total fluorescence yield and SLN retention must be considered when choosing an agent for eventual clinical use. Although the ultimate choice of contrast agent will depend on the specific clinical application, the following is a summary of the advantages and disadvantages of each:

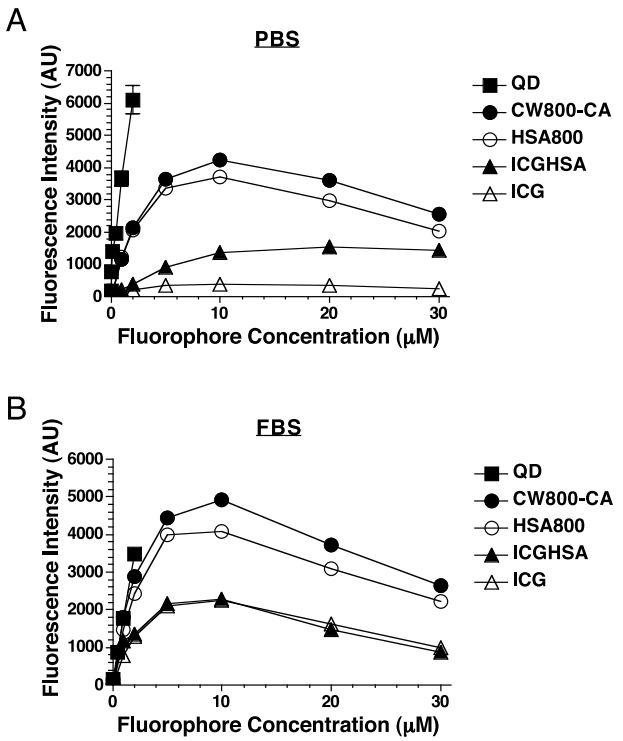

Figure 3. *The effects of fluorophore concentration and chemical environment on total fluorescence yield of 800 nm contrast agents in PBS (A) and in FBS (B).*

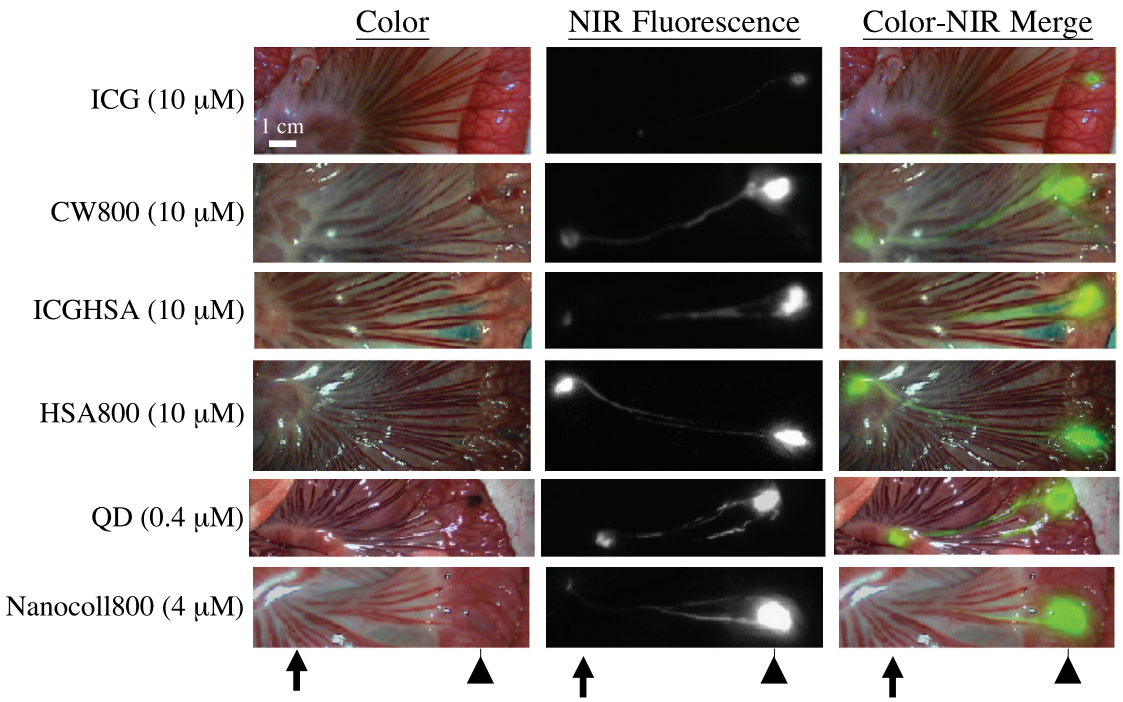

Figure 4. *Intraoperative NIR fluorescent SLN mapping of porcine intestine: 100 μl of each contrast agent, at the indicated concentration of fluorophore, was injected into the parenchyma of the porcine intestine (arrowheads) and followed to the SLN (arrows). Shown are color video (left), NIR fluorescence (middle), and a pseudocolored merged image of the two (right) 5 min after injection. NIR fluorescence images have identical exposure times (67 msec) and normalizations. SLN pixel values were within the linear range of the NIR camera.*

ICG: This molecule has been FDA-approved for other indications since 1958 and has an excellent safety profile [20,24–26]. Although ICG has been used previously for in vivo SLN mapping [27], its small hydrodynamic diameter results in rapid transport out of the SLN, its QY is highly dependent on local chemical environment, and its overall fluorescence yield is very low compared with other agents.

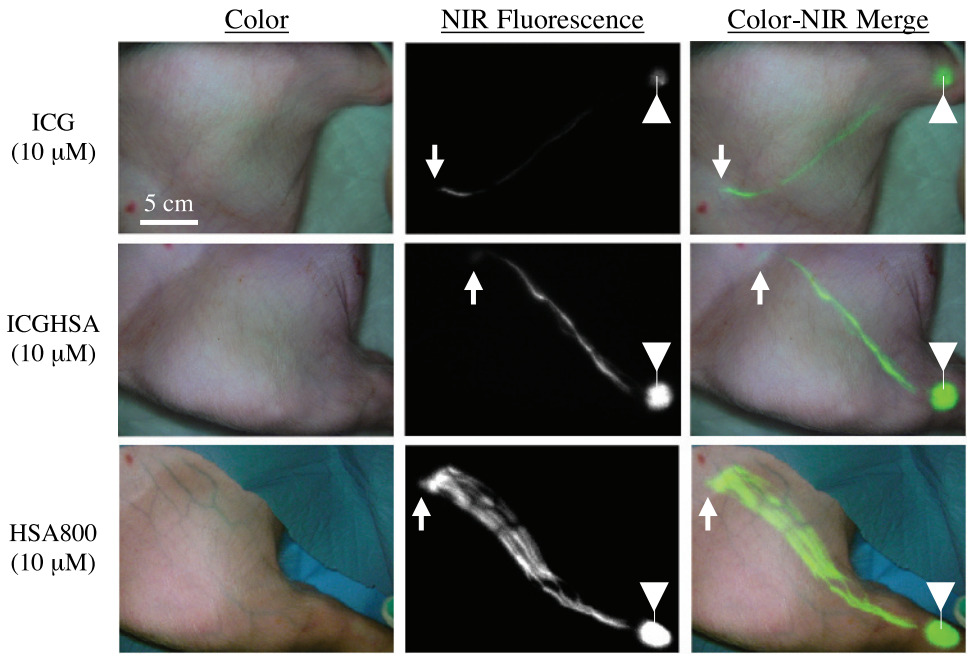

Figure 5. *Intraoperative NIR fluorescent SLN mapping of porcine limb: 300 μL of each contrast agent, at the indicated concentration of fluorophore, was injected intradermally in the foot (arrowheads) and followed to the SLN (arrows). Shown are color video (left), NIR fluorescence (middle), and a pseudocolored merged image of the two (right) 5 min after injection. NIR fluorescence images have identical exposure times (67 msec) and normalizations. SLN pixel values were within the linear range of the NIR camera.*

CW800-CA: The higher degree of sulfonation on this small molecule improves aqueous QY, reduces the effect of local environment, and improves SLN retention. However, hydrodynamic diameter is such that transport through the SLN is still a problem.

ICGHSA: The noncovalent adsorption of ICG to HSA improves its QY and results in a molecule with improved SLN retention. However, the improvement in total fluorescence yield becomes saturated beyond a 1:1 molar ratio of fluorophore to protein, and absolute affinity of the interaction is low [19,21,28,29], making it possible for dissociated ICG to travel through the SLN. Indeed, ICGHSA is quickly dissociated in vivo after passage through the liver (data not shown). The fluorescence yield and overall performance of ICGHSA was only twofold less than HSA800, making it a reasonable choice for clinical studies provided that an excitation fluence rate above 5 mW/cm^2 is utilized.

HSA800: This agent is a stable conjugate of highly fluorescent CW800 with HSA. Fluorescence yield has been maximized with respect to fluorophore substitution. Per-molecule fluorescence yield in serum is similar to QDs. Because anionic albumin is rapidly distributed to lymph [17,22,23], the highly anionic net charge of HSA800 might have contributed to its good SLN retention. However, its hydrodynamic diameter of 7.4 nm can still result in flow through the SLN, albeit at longer times than the small molecules ICG and CW800-CA. Practically speaking, HSA800 identifies the SLN unequivocally within seconds to minutes, and flow to distant lymph nodes can actually be used to assist with radical dissection in the presence of malignant cells in the SLN.

Nanocoll800: This agent is a derivative of human albumin nanocolloid, which is already used in Europe for radioscintigraphic SLN mapping [22,30]. Although the slow uptake and travel into lymphatics was expected, the degree of intra- and intermolecular quenching was surprising, and significantly limited the utility of this molecule (Figure 1B and C; Table 2). A significant advantage of this molecule, however, is that it is the only one to be fully retained by the SLN.

Once again, all agents were effective at identifying the SLN, however, some exhibited poor retention (ICG and CW800-CA), some had a low total fluorescence yield (ICG, Nanocoll800), most exhibited flow past the SLN after longer time points (all except Nanocoll800), and one had slow lymphatic uptake and transit (Nanocoll800). ICGHSA has the major advantage of being a mixture of two agents already FDA-approved for other indications, but exhibits a total fluorescence yield twofold less than HSA800. Hence, the choice of which organic alternative to QDs to use for initial SLN mapping clinical studies will depend on these many factors.

At this point in time, there is great debate about whether the SLN concept can be applied to solid tumors other than breast and melanoma. In colon cancer, for example, studies for [31] and against [32] its use have been published. The major criticism of all of these studies is that surgical proficiency with the technique has not been defined rigorously and objectively. Conventional SLN mapping technology is so complex that breast cancer SLN mapping requires a learning curve of at least 60 cases [4]. We hypothesize that the simplicity of our technology, and the fact that lymphatic flow can be followed in real time from the site of injection all the way to the SLN, will decrease and possibly eliminate the learning curve, and therefore reduce technical errors.

A second argument against SLN mapping in colon cancer and elsewhere is that SLN identification is not important if other loco-regional nodes are going to be resected anyway. This argument, however, ignores the clinical reality that a pathologist will only be able to make a cursory assessment of a large number of nodes, but will be able to subject the SLN to more rigorous ultra-staging. Once again, the ultimate utility of ultra-staging can only be assessed when the SLN technique itself has been optimized.

The major problem with optically based SLN mapping is depth sensitivity. One strategy is to employ frequency domain photon migration technology (reviewed in Refs. [6,7]), which theoretically could detect lymph nodes 4–10 cm below the surface. However, in many cases, even simple reflectance imaging (data herein) can be effective as the surgeon has the ability to follow lymphatic channels in real time, and if the channel dives deep into tissue, image-guided resection can be employed to follow it to the SLN.

In this study, we also present a general purpose algorithm for optimizing NIR fluorescent proteins for in vivo use. These robust methods complement our previous work on the development of NIR fluorescent small molecules and peptides [33]. The steps include determination of the mixing ratio to labeling ratio, the labeling ratio to per-fluorophore QY, the labeling ratio to total fluorescence yield, MALDI-TOF mass spectroscopic confirmation of fluorophore-labeled protein populations, and ES-TOF mapping of conjugation sites. For proteins that also have a particular bioactivity, the effect of labeling ratio on this activity must be measured separately, and the tradeoff among total fluorescence yield and bioactivity established. It is also of critical importance to measure the optical properties of NIR fluorescent proteins in both buffered saline as well as serum, because chemical environment can have a dramatic effect on spectral properties and QY. The photo-

bleaching threshold of heptamethine indocyanines, which is approximately 50 mW/cm^2 [34], was not an issue in the present study because fluence rate on surgical field was only 5 mW/cm^2. In this regard, NIR QDs remain the most robust of all SLN tracers, having remarkable photostability [11] and high fluorescence yield.

Finally, it should be emphasized that the absolute dose of organic NIR fluorescent contrast agent required for intraoperative SLN mapping using this technology is extremely low. Using 35-kg pigs, only 3 nmol (≈3 μg) of fluorophore was required for complete SLN mapping, image-guided resection, and high sensitivity inspection of the surgical field. This corresponds to only 3 nmol (200 μg) or 1 nmol (67 μg) of HSA protein for ICGHSA and HSA800, respectively. The human equivalent dose is only twofold higher than this, and corresponds to an albumin dose 50,000 times lower than that typically given intravenously for volume expansion. Most importantly, because both the injection site (tumor) and SLN are removed during the mapping procedure, the amount of contrast agent remaining in the body is minute.

Acknowledgments

We thank Daniel R. Draney, PhD (LI-COR) for providing CW800 derivatives and for many helpful discussions; Sang-Wook Kim, PhD and Moungi G. Bawendi, PhD (Massachusetts Institute of Technology) for providing NIR QDs; Alec M. De Grand for assistance with system software; Jaihyoung Lee, PhD for assistance with gel filtration chromatography; and Grisel Rivera for administrative assistance. This work was supported by Department of Energy (Office of Biological and Environmental Research) grant #DE-FG02-01ER63188, a Clinical Scientist Development Award from the Doris Duke Charitable Foundation (nonanimal experiments), an Application Development Award from the Center for Integration of Medicine and Innovative Technology (CIMIT), and grants #R21/33 CA-88245, #R21-CA-110185 (National Cancer Institute) and #R21/R33 EB-00673 (National Institute for Biomedical Imaging and Bioengineering) from the National Institutes of Health. Shunsuke Ohnishi received a Young Investigator Travel Award from the Society for Molecular Imaging (2004) and Ito Travel Foundation (2003).

References

[1] Morton DL, Wen DR, Wong JH, Economou JS, Cagle LA, Storm FK, Foshag LJ, Cochran AJ (1992). Technical details of intraoperative lymphatic mapping for early stage melanoma. *Arch Surg.* **127:**392–399.

[2] Schulze T, Bembenek A, Schlag PM (2004). Sentinel lymph node biopsy progress in surgical treatment of cancer. *Langenbeck's Arch Surg.* **389:**532–550.

[3] Cox CE, Pendas S, Cox JM, Joseph E, Shons AR, Yeatman T, Ku NN, Lyman GH, Berman C, Haddad F, Reintgen DS (1998). *Ann Surg.* **227:**645–651, discussion 651–653.

[4] Mariani G, Moresco L, Viale G, Villa G, Bagnasco M, Canavese G, Buscombe J, Strauss HW, Paganelli G (2001). Radioguided sentinel lymph node biopsy in breast cancer surgery. *J Nucl Med.* **42:**1198–1215.

[5] Schirrmeister H, Kotzerke J, Vogl F, Buck A, Czech N, Koretz K, Helm G, Kreienberg R, Kuhn T (2004). Prospective evaluation of factors influencing success rates of sentinel node biopsy in 814 breast cancer patients. *Cancer Biother Radiopharm.* **19:** 784–790.

[6] Sevick-Muraca EM, Houston JP, Gurfinkel M (2002). Fluorescence-enhanced, near infrared diagnostic imaging with contrast agents. *Curr Opin Chem Biol.* **6:**642–650.

[7] Ntziachristos V, Bremer C, Weissleder R (2003). Fluorescence imaging with near-infrared light: New technological advances that enable in vivo molecular imaging. *Eur Radiol.* **13:** 195–208.

[8] Frangioni JV (2003). In vivo near-infrared fluorescence imaging. *Curr Opin Chem Biol.* **7:**626–634.

[9] Nakayama A, del Monte F, Hajjar RJ, Frangioni JV (2002). Functional near-infrared fluorescence imaging for cardiac surgery and targeted gene therapy. *Molecular Imaging.* **1:**365–377.

[10] De Grand AM, Frangioni JV (2003). An operational near-infrared fluorescence imaging system prototype for large animal surgery. *Technol Cancer Res Treat.* **2:**553–562.

[11] Kim S, Lim YT, Soltesz EG, De Grand AM, Lee J, Nakayama A, Parker JA, Mihaljevic T, Laurence RG, Dor DM, Cohn LH, Bawendi MG, Frangioni JV (2004). Near-infrared fluorescent type II quantum dots for sentinel lymph node mapping. *Nat Biotechnol.* **22:**93–97.

[12] Soltesz EG, Kim S, Laurence RG, DeGrand AM, Parungo CP, Dor DM, Cohn LH, Bawendi MG, Frangioni JV, Mihaljevic T (2005). Intraoperative sentinel lymph node mapping of the lung using near-infrared fluorescent quantum dots. *Ann Thorac Surg.* **79:**269–277, discussion 269–277.

[13] Parungo CP, Ohnishi S, Kim SW, Kim SJ, Laurence RG, Soltesz EG, Chen FY, Colson YL, Cohn LH, Bawendi MG, Frangioni JV (2005). Intraoperative identification of esophageal sentinel lymph nodes using near-infrared fluorescence imaging. *J Thor Cardiovasc Surg.* **129:**844–850.

[14] Parungo CP, Colson YL, Kim S, Kim S, Cohn LH, Bawendi MG, Frangioni JV (2005). Sentinel lymph node mapping of the pleural space. *Chest.* **127:**1799–1804.

[15] Frangioni JV, Kim SW, Ohnishi S, Bawendi MG (In press). Sentinel lymph node mapping with type II quantum dots. *Methods Mol Biol.*

[16] Fujii H, Kitagawa Y, Kitajima M, Kubo A (2004). Sentinel nodes of malignancies originating in the alimentary tract. *Ann Nucl Med.* **18:**1–12.

[17] Swart PJ, Beljaars L, Kuipers ME, Smit C, Nieuwenhuis P, Meijer DK (1999). Homing of negatively charged albumins to the lymphatic system: General implications for drug targeting to peripheral tissues and viral reservoirs. *Biochem Pharmacol.* **58:**1425–1435.

[18] Josephson L, Mahmood U, Wunderbaldinger P, Tang Y, Weissleder R (2003). Pan and sentinel node lymph nodes visualization using a near infrared fluorescent probe. *Mol Imaging.* **2:**18–23.

[19] Moody ED, Viskari PJ, Colyer CL (1999). Non-covalent labeling of human serum albumin with indocyanine green: A study by capillary electrophoresis with diode laser-induced fluorescence detection. *J Chromatogr B Biomed Sci Appl.* **729:**55–64.

[20] Benson C, Kues HA (1977). Absorption and fluorescence properties of cyanine dyes. *J Chem Eng Data.* **22:**379–383.

[21] Sauda K, Imasaka T, Ishibashi N (1986). Determination of protein in human serum by high-performance liquid chromatography with semiconductor laser fluorometric detection. *Anal Chem.* **58:**2649–2653.

[22] Szuba A, Shin WS, Strauss HW, Rockson S (2003). The third

circulation: Radionuclide lymphoscintigraphy in the evaluation of lymphedema. *J Nucl Med.* **44:**43–57.

[23] Mangat S, Patel HM (1985). Lymph node localization of non-specific antibody-coated liposomes. *Life Sci.* **36:**1917–1925.

[24] Regillo CD (1999). The present role of indocyanine green angiography in ophthalmology. *Curr Opin Ophthalmol.* **10:** 189–196.

[25] Henschen S, Busse MW, Zisowsky S, Panning B (1993). Determination of plasma volume and total blood volume using indocyanine green: A short review. *J Med.* **24:**10–27.

[26] Burra P, Masier A (2004). Dynamic tests to study liver function. *Eur Rev Med Pharmacol Sci.* **8:**19–21.

[27] Reynolds JS, Troy TL, Mayer RH, Thompson AB, Waters DJ, Cornell KK, Snyder PW, Sevick-Muraca EM (1999). Imaging of spontaneous canine mammary tumors using fluorescent contrast agents. *Photochem Photobiol.* **70:**87–94.

[28] Sowell J, Agnew-Heard KA, Mason JC, Mama C, Strekowski L, Patonay G (2001). Use of non-covalent labeling in illustrating ligand binding to human serum albumin via affinity capillary electrophoresis with near-infrared laser induced fluorescence detection. *J Chromatogr B Biomed Sci Appl.* **755:**91–99.

[29] Williams RJ, Lipowska M, Patonay G, Strekowski L (1993). Comparison of covalent and noncovalent labeling with near-infrared dyes for the high-performance liquid chromatographic determination of human serum albumin. *Anal Chem.* **65:** 601–605.

[30] Schlag PM, Bembenek A, Schulze T (2004). Sentinel node biopsy in gastrointestinal-tract cancer. *Eur J Cancer.* **40:**2022–2032.

[31] Paramo JC, Summerall J, Poppiti R, Mesko TW (2002). Validation of sentinel node mapping in patients with colon cancer. *Ann Surg Oncol.* **9:**550–554.

[32] Bertagnolli M, Miedema B, Redston M, Dowell J, Niedzwiecki D, Fleshman J, Bem J, Mayer R, Zinner M, Compton C (2004). Sentinel node staging of resectable colon cancer: Results of a multicenter study. *Ann Surg.* **240:**624–628, discussion 628–630.

[33] Zaheer A, Wheat TE, Frangioni JV (2002). IRDye78 conjugates for near-infrared fluorescence imaging. *Mol Imaging.* **1:**354–364.

[34] Nakayama A, Bianco AC, Zhang CY, Lowell BB, Frangioni JV (2003). Quantitation of brown adipose tissue perfusion in transgenic mice using near-infrared fluorescence imaging. *Mol Imaging.* **2:**37–49.